ACS APPLIED MATERIALS & INTERFACES

Letter

www.acsami.org

Photocatalytic Activity of Hydrogenated TiO_2

Tim Leshuk,[†] Roozbeh Parviz,[‡] Perry Everett,[†] Harish Krishnakumar,[†] Robert A. Varin,[‡,§] and Frank Gu*[,†,§]

[†]Department of Chemical Engineering, [‡]Department of Mechanical and Mechatronics Engineering, and [§]Waterloo Institute for Nanotechnology, University of Waterloo, Waterloo, Ontario, Canada

Supporting Information

ABSTRACT: Photocatalysis is a promising advanced water treatment technology, and recently the possibility of using hydrogenation to improve the photocatalytic efficiency of titanium dioxide has generated much research interest. Herein we report that the use of high-temperature hydrogenation to prepare black TiO_2 primarily results in the formation of bulk defects in the material without affecting its electronic band structure. The hydrogenated TiO_2 exhibited significantly worse photocatalytic activity under simulated sunlight compared to the unhydrogenated control, and thus we propose that high-temperature hydrogenation can be counterproductive to improving the photocatalytic activity of TiO_2, because of its propensity to form bulk vacancy defects.

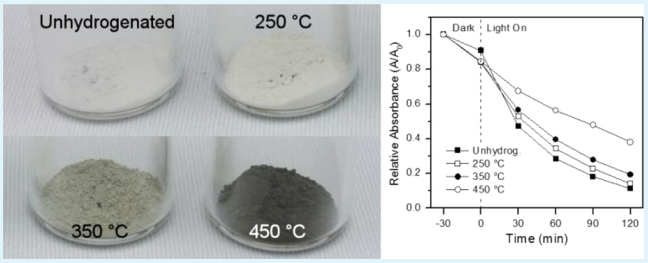

KEYWORDS: *TiO_2, photocatalysis, hydrogenation, defects, visible light, trap states*

Photocatalysis over titanium dioxide has been heavily investigated as a promising means of treating a wide variety of emerging pollutants,[1−7] and recent research effort has been devoted to improving the photocatalytic efficiency of TiO_2 through a variety of materials engineering approaches, such as improving charge carrier separation and utilization by cocatalyst immobilization or controlled faceting,[8−13] or enhancing the visible-light activity of TiO_2 through doping.[4,14−16] Recently Chen et al. reported a novel technique that apparently combined these two approaches, wherein black hydrogenated TiO_2 nanocrystals exhibited strong visible light absorbance, a disordered surface enriched in trap states, and remarkably improved solar photocatalytic performance.[17] Since this initial report, several theoretical and experimental studies on the hydrogenation of TiO_2 have been published;[18−31] however, most of these works have explored applications other than photocatalysis, and the dramatic hydrogenation-induced improvement in TiO_2 photocatalytic activity initially reported by Chen et al. has not been elucidated. Specifically, many of the studies reported so far have used high-temperature ($T > 673$ K) hydrogenation treatments of TiO_2.[22−28,31] Herein, we report that high-temperature hydrogenation, although shown to be beneficial for other applications, can serve to degrade the photocatalytic performance of TiO_2 in water decontamination.

For well-controlled particle geometry and gas permeation, we coated substrate silica spheres with a uniform and highly porous nanocrystalline anatase TiO_2 shell through standard sol−gel chemistry (see Figure S1a and Supporting Information). Prior to hydrogenation, these particles were extensively calcined in air in order to completely remove the surfactant used during particle synthesis, and to crystallize the TiO_2 in the hopes of confining hydrogen-induced material transformation to the surface of the TiO_2 nanoparticles. These particles were then kept at various temperatures (250, 350, and 450 °C) under 20 bar H_2 for 24 h. Following hydrogenation, the powders, originally pure white in color, were observed to exhibit obvious and strong visible light absorbance, progressing from a very pale yellow through gray to black with increasing hydrogenation temperature (Figure 1a). This coloration remained stable over time with exposure of the particles to air or water.[28]

UV/vis spectroscopy revealed that the hydrogenation treatment at temperatures less than 450 °C did not change the bandgap of the particles, which remained at ∼3.45 eV, somewhat larger than the typical bandgap of ∼3.2 eV reported for anatase TiO_2,[3] likely due to the silica substrate effect (see Figure S2 in the Supporting Information).[32] Although the UV/vis spectrum for the 450 °C sample was difficult to interpret, as these particles exhibited strong absorbance throughout the visible range, apparently the bandgap of these particles also remained essentially unchanged from the unhydrogenated control. These results would seem to indicate that the hydrogenation induced visible-light absorption (i.e., the increased broad absorption of the 450 °C sample in the visible range, see Figure S2 in the Supporting Infomration) is due primarily to an increase in interband states in the TiO_2, as has been reported previously,[22,23,29,30] rather than a shift in the position of either band edge as typically occurs as a result of doping.[3,33−36]

Received: November 29, 2012
Accepted: March 6, 2013
Published: March 6, 2013

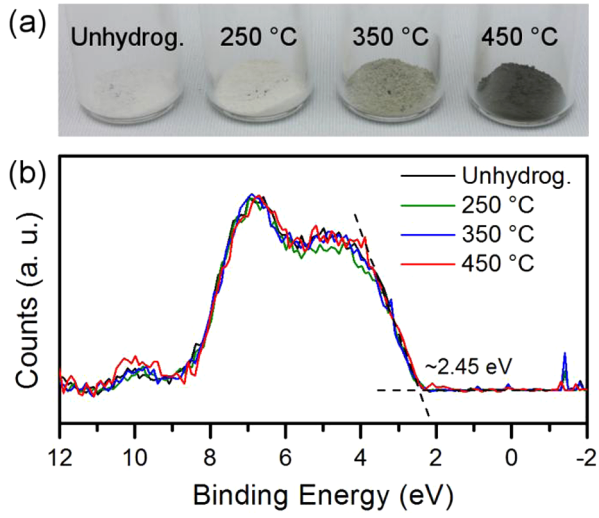

Figure 1. (a) Photograph and (b) valence band XPS spectra of the powders after hydrogenation at the indicated temperatures for 24 h.

XRD characterization revealed that the TiO_2 crystallinity was well preserved though the hydrogenation treatment, and the peaks could be readily indexed to the anatase phase (see Figure S3 in the Supporting Information). These results are similar to other recent studies that have found that the bulk lattice structure of TiO_2 remains largely unchanged following hydrogenation (where the term "bulk" herein refers to the noninterfacial/subsurface TiO_2 within the nanocrystals).[17,26,27,30,31] No significant change in the morphology of the TiO_2 shell was observed on TEM (see Figure S1b in the Supporting Information).

XPS revealed no unusual features in the Ti 2p region, nor any differences between any of the samples before or after hydrogenation, where the Ti $2p_{3/2}$ peak position of 458.4 eV is characteristic of Ti^{4+} in TiO_2 (see Figure S4a in the Supporting Information).[17,22,26,37] This is not surprising, as any Ti^{3+} which may have been present at the particle surface would have been readily oxidized on exposure of the samples to air.[26,38]The O 1s region was very similar for the samples before and after hydrogenation, albeit with some minor variations (see Figure S4b in the Supporting Information). The O 1s spectra could be deconvoluted into three component peaks (see Figure S4c in the Supporting Information), wherein the lowest energy peak (529.7 eV) was assigned to lattice oxygen in TiO_2 (O_L), the highest energy peak to lattice oxygen in silica (533.2 eV), and a broad middle peak (531.9 eV) corresponding to Ti−OH surface hydroxyl species (O_{OH}).[22,32] The total Ti:O ratio did not vary significantly between the samples, although the O_{OH}:O_L ratio increased by approximately 20% from the unhydrogenated control to the 450 °C hydrogenated sample (see Table S1 in the Supporting Information), indicating that the surface stoichiometry of the TiO_2 remained relatively unchanged as a result of hydrogenation, apart from a small increase in the concentration of surface hydroxyl groups, possibly formed through the H_2 induced breaking of bridging Ti−O−Ti bonds.[30] Notably, however, the increase in Ti−OH content after hydrogenation was not nearly as significant as reported by Chen et al.[17] Perhaps most importantly, the valence band XPS spectra remained virtually identical for all the samples before and after hydrogenation (Figure 1b), confirming the UV/vis bandgap results, whereas a dramatic shift of the valence band edge by ∼2.18 eV due to introduction of band tail states was a defining feature of the black TiO_2 particles in the report by Chen et al.[17] This lack of any change to the valence band as a result of high temperature hydrogenation was also recently observed by Wang et al.[23]

Raman spectroscopy revealed significant peak broadening and shifting as a result of hydrogenation (Figure 2a and Figure S5a in the Supporting Information), as well as the appearance of a strong new peak at 1354 cm^{-1} in the 450 °C sample (see Figure S5b in the Supporting Information), which is attributed to a Ti−H mode.[39] The peak broadening effect and shift has been observed in several recent studies on hydrogenated TiO_2, and is attributed to the presence of lattice disorder resulting from phonon confinement or nonstoichiometry as a result of oxygen vacancy (V_O) doping.[22,33,40,41] However, the appearance of unidentifiable Raman bands after hydrogenation, associated with TiO_2 surface disordering,[17] were not observed. The conclusion drawn from the sum of these characterizations is that the strong visible-light absorption of the hydrogenated samples is due to bulk V_O doping of the TiO_2 rather than any significant shift in band edge position or change in surface structure.

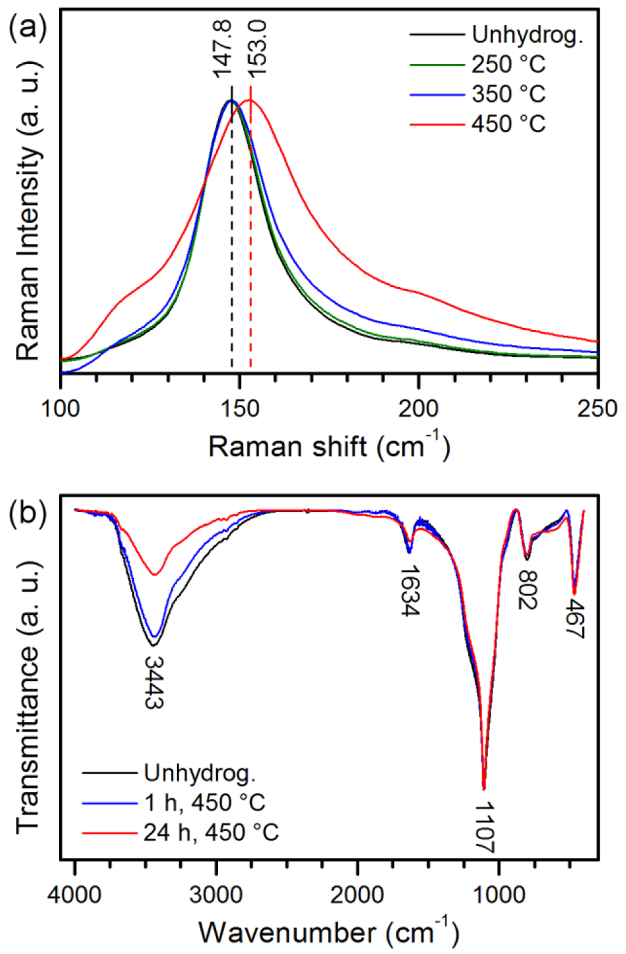

Figure 2. (a) Raman spectra of the primary E_g mode in the samples after hydrogenation at the indicated temperature for 24 h. (b) FTIR spectra of the samples after hydrogenation at 450 °C for the times indicated.

We tested the activity of the particles as photocatalysts in the degradation of methylene blue, a standard model contaminant, in water under simulated sunlight, the results of which are

dx.doi.org/10.1021/am302903n | ACS Appl. Mater. Interfaces 2013, 5, 1892−1895

presented in Figure 3. As is readily observed, the photocatalytic activity of the particles under the test conditions was

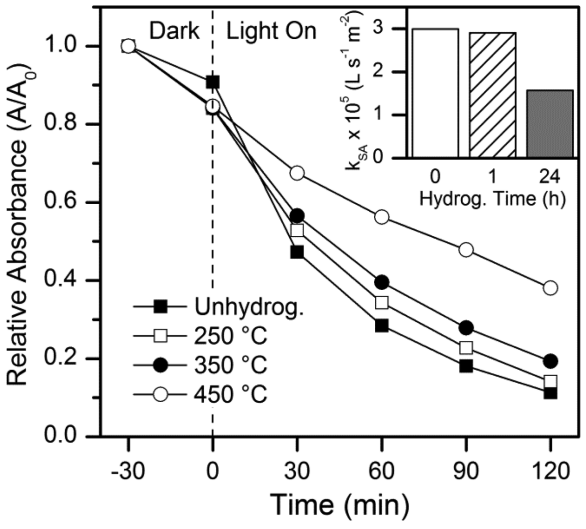

Figure 3. Photocatalytic decolouration of aqueous methylene blue (MetB, 5 mg L^{-1}) under simulated sunlight with 0.05 g L^{-1} catalyst particles hydrogenated at the indicated temperatures for 24 h. Inset: surface area normalized pseudofirst order rate constant (k_{SA}) comparison for the samples hydrogenated at 450 °C for the indicated times, tested under the same conditions.

substantially degraded as a result of hydrogenation treatment, where the photocatalytic dye degradation rate decreased with increasing hydrogenation temperature.[17] To identify a cause of this hydrogenation induced decrease in photocatalytic activity, we characterized the specific surface area of the samples before and after hydrogenation, as we suspected that the 24 h treatment at 450 °C could have resulted in significant decrease in the surface area of the particles due to nanocrystal growth through sintering in the TiO_2 shell, which would obviously adversely affect photocatalytic activity. Indeed, hydrogenation at 450 °C for 24 h decreased the specific surface area of the powder by ~67% relative to the unhydrogenated control (see Table S2 in the Supporting Information). This loss in surface area was correlated with a decrease in the intensity of IR-active hydroxyl vibrational modes at ~3443 and ~1634 cm^{-1} (Figure 2b), likely due to elimination of internal hydroxyls from within the TiO_2 shell resulting from pore collapse during the hydrogenation treatment, as XPS had detected a slight increase in surface hydroxyl content for the 450 °C sample, as discussed above.

To counteract this loss in surface area, a sample was also prepared by hydrogenation at 450 °C for only 1 h for comparison. The loss in surface area and associated hydroxyl content was more moderate for this sample (see Table S2 in the Supporting Information and Figure 2b). However, when subjected to the same photocatalytic test as above, the photocatalytic degradation rate of the hydrogenated samples, even normalized for surface area, was still not significantly different than the unhydrogenated control, and the activity of the 24 h black hydrogenated sample was substantially worse (Figure 3 inset).

We therefore attribute this loss in photocatalytic activity primarily to bulk V_O doping of the TiO_2 as a result of hydrogenation. These intraband defect states, while allowing for strong optical absorbance throughout the visible range, have previously been shown to be photocatalytically inactive.[23] Furthermore, as the vacancy defects are confined to the core of the TiO_2 crystals rather than their surface, they are more likely to behave as trap states and charge carrier recombination centers.[37,42] Thus the observed increase in visible-light absorbance and concomitant decrease in photocatalytic activity is purported to be due to an increase in the concentration of V_O defects in the TiO_2 lattice with increasing hydrogenation temperature.

Although the increase in the conductivity of TiO_2 that V_O doping provides has been demonstrated to be helpful in some applications,[23,24] we show that hydrogenation-induced bulk defects can significantly degrade photocatalytic activity for water remediation.[42] As the characterization results reported herein are highly similar to a number of recent studies carrying out high-temperature hydrogenations of TiO_2, and significantly different from the original study by Chen et al.,[17] we propose that high-temperature hydrogenation is the wrong approach to attempt to increase TiO_2 photocatalytic activity, as high temperatures are more likely to induce bulk vacancy defects. We recommend therefore that future research focus rather on the unique hydrogenation-induced surface disorder layer reported by Chen et al. and its formation mechanism.[17,22,42,43]

For example, Jiang et al. have recently shown that vacancies near the hydrogenation-disordered surface can enhance photocatalytic activity through charge carrier trapping and prevention of recombination.[43] Similarly, Xia and Chen have recently shown that anatase nanocrystals with predominant (102) facets, rather than the typical (101) facets of anatase, undergo a unique surface transformation upon low-temperature hydrogenation.[44] However, as shown herein, generation of black TiO_2 at lower hydrogenation temperatures is not a general phenomenon, and thus alternative synthesis and hydrogenation strategies must be explored in order to generalize and advance the promising photocatalytic results of the black hydrogenated TiO_2 reported by Chen et al.

■ ASSOCIATED CONTENT

Supporting Information

Synthesis, characterization and testing methods, and additional characterization figures and data, including TEM, UV/vis, XRD, XPS, Raman, and BET. This material is available free of charge via the Internet at http://pubs.acs.org.

■ AUTHOR INFORMATION

Corresponding Author

*E-mail: frank.gu@uwaterloo.ca.

Notes

The authors declare no competing financial interests.

■ ACKNOWLEDGMENTS

This work was financially supported by Natural Sciences and Engineering Research Council of Canada.

■ REFERENCES

(1) Chong, M. N.; Jin, B.; Chow, C. W. K.; Saint, C. *Water Res.* **2010**, *44*, 2997−3027.
(2) Malato, S.; Fernandez-Ibanez, P.; Maldonado, M. I.; Blanco, J.; Gernjak, W. *Catal. Today* **2009**, *147*, 1−59.
(3) Henderson, M. A. *Surf. Sci. Rep.* **2011**, *66*, 185−297.
(4) Asahi, R.; Morikawa, T.; Ohwaki, T.; Aoki, K.; Taga, Y. *Science* **2001**, *293*, 269−271.

(5) Dalrymple, O. K.; Yeh, D. H.; Trotz, M. A. *J. Chem. Technol. Biotechnol.* **2007**, *82*, 121−134.
(6) Dimitroula, H.; Daskalaki, V. M.; Frontistis, Z.; Kondarides, D. I.; Panagiotopoulou, P.; Xekoukoulotakis, N. P.; Mantzavinos, D. *Appl. Catal., B* **2012**, *117*, 283−291.
(7) Gueltekin, I.; Ince, N. H. *J. Environ. Manage.* **2007**, *85*, 816−832.
(8) Yang, H. G.; Sun, C. H.; Qiao, S. Z.; Zou, J.; Liu, G.; Smith, S. C.; Cheng, H. M.; Lu, G. Q. *Nature* **2008**, *453*, 638−U4.
(9) Pan, J.; Liu, G.; Lu, G. Q.; Cheng, H. *Angew. Chem., Int. Ed.* **2011**, *50*, 2133−2137.
(10) Zhang, J.; Xiong, Z.; Zhao, X. S. *J. Mater. Chem.* **2011**, *21*, 3634−3640.
(11) Liu, G.; Yu, J. C.; Lu, G. Q.; Cheng, H. *Chem. Commun.* **2011**, *47*, 6763−6783.
(12) Zhang, Q.; Lima, D. Q.; Lee, I.; Zaera, F.; Chi, M.; Yin, Y. *Angew. Chem., Int. Ed.* **2011**, *123*, 7226−7230.
(13) Gomes Silva, C.; Juarez, R.; Marino, T.; Molinari, R.; Garcia, H. *J. Am. Chem. Soc.* **2011**, *133*, 595−602.
(14) Yu, H.; Irie, H.; Hashimoto, K. *J. Am. Chem. Soc.* **2010**, *132*, 6898−6899.
(15) Li, Z.; Shi, F.; Zhang, T.; Wu, H.; Sun, L.; Yan, C. *Chem. Commun.* **2011**, *47*, 8109−8111.
(16) Liu, R.; Wang, P.; Wang, X.; Yu, H.; Yu, J. *J. Phys. Chem. C* **2012**, *116*, 17721−17728.
(17) Chen, X.; Liu, L.; Yu, P. Y.; Mao, S. S. *Science* **2011**, *331*, 746−750.
(18) Syzgantseva, O. A.; Gonzalez-Navarrete, P.; Calatayud, M.; Bromley, S.; Minot, C. *J. Phys. Chem. C* **2011**, *115*, 15890−15899.
(19) Lu, J.; Dai, Y.; Jin, H.; Huang, B. *Phys. Chem. Chem. Phys.* **2011**, *13*, 18063−18068.
(20) Pan, H.; Zhang, Y.; Shenoy, V. B.; Gao, H. *J. Phys. Chem. C* **2011**, *115*, 12224−12231.
(21) Li, M.; Zhang, J.; Guo, D.; Zhang, Y. *Chem. Phys. Lett.* **2012**, *539*, 175−179.
(22) Naldoni, A.; Allieta, M.; Santangelo, S.; Marelli, M.; Fabbri, F.; Cappelli, S.; Bianchi, C. L.; Psaro, R.; Dal Santo, V. *J. Am. Chem. Soc.* **2012**, *134*, 7600−7603.
(23) Wang, G.; Wang, H.; Ling, Y.; Tang, Y.; Yang, X.; Fitzmorris, R. C.; Wang, C.; Zhang, J. Z.; Li, Y. *Nano Lett.* **2011**, *11*, 3026−3033.
(24) Lu, X.; Wang, G.; Zhai, T.; Yu, M.; Gan, J.; Tong, Y.; Li, Y. *Nano Lett.* **2012**, *12*, 1690−1696.
(25) Shin, J.; Joo, J. H.; Samuelis, D.; Maier, J. *Chem. Mater.* **2012**, *24*, 543−551.
(26) Hoang, S.; Berglund, S. P.; Hahn, N. T.; Bard, A. J.; Mullins, C. B. *J. Am. Chem. Soc.* **2012**, *134*, 3659−3662.
(27) Sun, C.; Jia, Y.; Yang, X.; Yang, H.; Yao, X.; Lu, G. Q.; Selloni, A.; Smith, S. C. *J. Phys. Chem. C* **2011**, *115*, 25590−25594.
(28) Danon, A.; Bhattacharyya, K.; Vijayan, B. K.; Lu, J.; Sauter, D. J.; Gray, K. A.; Stair, P. C.; Weitz, E. *ACS Catal* **2012**, *2*, 45−49.
(29) Wang, W.; Lu, C.; Ni, Y.; Song, J.; Su, M.; Xu, Z. *Catal. Commun.* **2012**, *22*, 19−23.
(30) Wei, W.; Yaru, N.; Chunhua, L.; Zhongzi, X. *RSC Adv.* **2012**, *2*, 8286−8288.
(31) Zheng, Z.; Huang, B.; Lu, J.; Wang, Z.; Qin, X.; Zhang, X.; Dai, Y.; Whangbo, M. *Chem. Commun.* **2012**, *48*, 5733−5735.
(32) Gao, X.; Wachs, I. *Catal. Today* **1999**, *51*, 233−254.
(33) Chen, X.; Mao, S. S. *Chem. Rev.* **2007**, *107*, 2891−2959.
(34) Fujishima, A.; Zhang, X.; Tryk, D. A. *Surf. Sci. Rep.* **2008**, *63*, 515−582.
(35) Zuo, F.; Bozhilov, K.; Dillon, R. J.; Wang, L.; Smith, P.; Zhao, X.; Bardeen, C.; Feng, P. *Angew. Chem., Int. Ed.* **2012**, *51*, 6223−6226.
(36) Zuo, F.; Wang, L.; Wu, T.; Zhang, Z.; Borchardt, D.; Feng, P. *J. Am. Chem. Soc.* **2010**, *132*, 11856−11857.
(37) Xiong, L.; Li, J.; Yang, B.; Yu, Y. *J. Nanomater.* **2012**, 831524.
(38) Guillemot, F.; Porte, M.; Labrugere, C.; Baquey, C. *J. Colloid Interface Sci.* **2002**, *255*, 75−78.
(39) Turkovic, A.; Ivanda, M.; Drasner, A.; Vranesa, V.; Persin, M. *Thin Solid Films* **1991**, *198*, 199−205.
(40) Venkatasubbu, G. D.; Ramakrishnan, V.; Sasirekha, V.; Ramasamy, S.; Kumar, J. *J. Exp. Nanosci.* **2012**, *0*, 1−8.
(41) Zhang, W.; He, Y.; Zhang, M.; Yin, Z.; Chen, Q. *J. Phys. D: Appl. Phys.* **2000**, *33*, 912−916.
(42) Kong, M.; Li, Y.; Chen, X.; Tian, T.; Fang, P.; Zheng, F.; Zhao, X. *J. Am. Chem. Soc.* **2011**, *133*, 16414−16417.
(43) Jiang, X.; Zhang, Y.; Jiang, J.; Rong, Y.; Wang, Y.; Wu, Y.; Pan, C. *J. Phys. Chem. C* **2012**, *116*, 22619−22624.
(44) Xia, T.; Chen, X. *J. Mater. Chem. A* **2013**, *1*, 2983−2989.